Optimum information in crackling noise

Chunsheng Lu,[1,*] Yiu-Wing Mai,[1] and Yao-Gen Shen[2]
[1]*Centre for Advanced Materials Technology (CAMT), School of Aerospace, Mechanical and Mechatronic Engineering J07, The University of Sydney, Sydney, NSW 2006, Australia*
[2]*Department of Manufacturing Engineering and Engineering Management (MEEM), City University of Hong Kong, Kowloon, Hong Kong, China*
(Received 22 December 2004; published 8 August 2005)

The crackling noise due to scratching superhard nanocomposite coatings was investigated by using a simple stick-slip model. The optimum information extracted from statistical analysis, in terms of the Akaike information criterion, is in good agreement with real tests. As a nanocomposite coating approaches an optimal performance, the acoustic emission energy follows a power-law distribution and its behavior is likely to be independent of microscopic and macroscopic details. The results imply that a peculiar deformation behavior, due to the competition between different deformation mechanisms such as dislocation pileups in nanocrystalline grains and grain sliding-grain rotation within amorphous boundaries, plays a vital role in the nanostructure with superhardness.

DOI: 10.1103/PhysRevE.72.027101 PACS number(s): 62.20.Qp, 05.40.−a, 81.07.−b

When crumpling a piece of paper, we can hear intermittent, and sometimes, sharp noises. In fact, almost all the systems crackle as a response to external excitations. These systems usually span a broad range of spatiotemporal scales, from tiny damage of materials at the micrometer or nanometer scale to large tremors of tectonic plates at the huge scale and, even, to price fluctuations in stock markets. Intuitively, the more we learn about crackling noise, the more complex it appears. Interest in crackling noise may go back several decades, but rapid progress in this multidisciplinary field has been made in the last decade or so partially due to new discoveries in statistical physics [1]. For instance, the size distribution of crackling noise in many systems often follows power-law (fractal) statistics without characteristic length scales. More importantly, crackling noise in diverse systems that at first sight may seem unrelated often shares some common features, which are likely independent of microscopic and macroscopic details [1–4]. The description of large-scale behaviors can be made by simple models which rely on only a few emergent parameters. A well-known example is the self-organized criticality model for the explanation of $1/f$ noise in the avalanche of sandpiles, which inspired much of the succeeding work on crackling noise in different systems [5].

As the response record of a system on external excitations, crackling noise should include much more useful information than what we have known. Here one of the most important challenges is to make a quantitative comparison between theoretical models and experimental results and, further, to make the study of crackling noise profitable [1]. In this Brief Report, such an endeavor has been made by applying a simple statistical stick-slip model to acoustic emission (AE) signals, a typical kind of crackling noise, caused by scratching superhard nanocomposite coatings (with Vickers hardness $H \geqslant 40$ GPa, and for comparison, the hardness of diamond is about 100 GPa). We will focus our attention on whether some optimum information could be extracted from the crackling noise and its implications for a better understanding of the superhardening mechanisms of nanocomposite coatings.

Among a large number of hard materials, there are only a few truly superhard materials available, and their superhardening mechanisms are still unclear [6]. To evaluate the integrity of superhard nanocomposite coatings, the scratching test is a simple and convenient method. However, the tribological properties of these coatings are rather complicated and influenced by many factors over multiscales, such as cracking, delamination, buckling, etc. [7–10]. Fortunately, these factors can be directly monitored by an AE sensor because the nucleation and growth of dislocations or cracks result in a sudden change in stress or displacement within a solid in the form of elastic waves with ultrasonic frequencies [7,8].

Figure 1 shows typical results from standard scratching tests of superhard nc-TiN/a-Si_3N_4 coatings deposited onto an M42 high-speed-steel substrate. "nc" and "a" represent nanocrystalline and amorphous phases, respectively. A Rockwell C diamond indenter tip (200 μm in radius) was drawn across the coating surface at a constant linear velocity of 10 mm min^{-1} while increasing the load from 10 to 70 N at a constant rate of 100 N min^{-1}. It is obvious that, as time t increases, the fluctuation of friction force F_t increases and the first derivative of AE (dF_t/dt) becomes rougher. There are two time scales in this process: the characteristic relaxation time τ and the measuring time T. Their ratio—that is, the Deborah number $\mathrm{De}=\tau/T \ll 1$—means that the coating subjected to scratching exhibits a "liquidlike" behavior. A recent experiment provided evidence of a ductile fracture mode on the nanometer scale in a vitreous material at a temperature much lower than the glass transition temperature [11]. This behavior can be easily described by a stick-slip process that occurs in most sliding friction phenomena in various materials [9,10]. Here it is assumed that the stress (or energy) level in a coating can be described by using a scalar

*Electronic address: chunsheng.lu@aeromech.usyd.edu.au

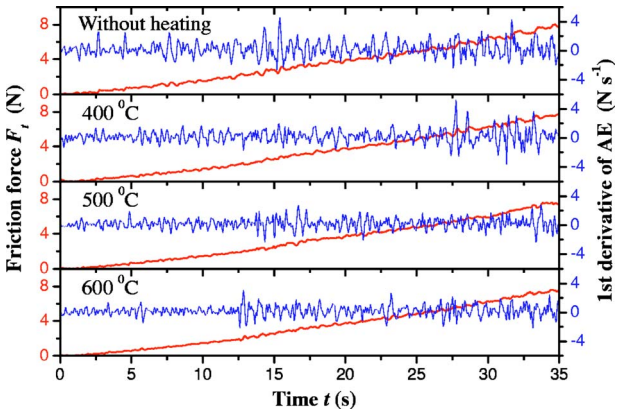

FIG. 1. (Color online) Typical tribological properties from scratching nc-TiN/a-Si_3N_4 coatings (8.6 at. % Si) deposited on M42 high-speed-steel substrates at different temperatures. Here the friction force F_t is the product of normal force by the coefficient of friction and the first derivative of acoustic emission is the differential of the friction force F_t to time t.

value $\sigma(t)$, which increases deterministically between AE events and releases stochastically as a Markov process. Thus the evolution of stress is given by

$$\sigma(t) = \sigma(0) + \rho t - S(t), \tag{1}$$

where $\sigma(0)$ is initial stress level, ρ is constant external loading rate, and $S(t)=\Sigma_{i:t_i<t}S_i(t)$ is the accumulated stress release from events within the region over the time period $(0,t)$, where t_i and S_i are the origin time and stress release associated with the ith AE event, respectively [12]. The value of stress release during an AE event can be estimated from its magnitude m in terms of the empirical formula

$$m = 10 \log_{10} A + \text{const}, \tag{2}$$

where the unit of m is decibel (dB) and A is relative strength of an AE signal, such as power, voltage, etc. For simplicity, the stress drop in an AE event is approximately proportional to its strength. Thus we have $S_i=10^{0.1(m_i-m_0)}$, where m_0 is the reference magnitude and $m_0=60$ dB was used in subsequent analysis (and the noise level of normal conversation is $\sim$60 dB) [8]. It is worth noting that the substance of results is not sensitive to the choice of m_0 [12].

The probability intensity of an AE occurrence in a coating is controlled by a risk function $\psi(\sigma)$, which increases nonlinearly with the stress level σ. The simplest choice of $\psi(\sigma)$ is taken as an exponential function $\psi(\sigma)=\exp(\mu+\nu\sigma)$, where μ and ν represent the background and sensitivity to risk, respectively. This is a compromise between time-predictable and pure random (Poisson) processes [13]. It is further assumed that the size distribution of AE events is independent of stress level, and the AE signals from scratch tests can be treated as a marked point process in a time-stress space with the conditional intensity function:

$$\lambda(t) = \psi[\sigma(t)] = \exp\{\alpha + \nu[\rho t - S(t)]\}, \tag{3a}$$

where α $[=\mu+\nu\sigma(0)]$, ν, and ρ are adjustable fitting parameters. To remove the influence of sample size (the number of AE events), Eq. (3a) can be rewritten as

$$\bar{\lambda}(t) = \lambda(t)\exp(-\alpha) = \exp\left\{\eta\left[\frac{t}{t_0} - \frac{S(t)}{S_0}\right]\right\}, \tag{3b}$$

where $\eta=\nu S_0$, $t_0=S_0/\rho$, and $S_0=\Sigma S_i/N$. Here N is number of AE events over the observation interval (t_1,t_2). Estimates of these parameters are found by maximizing its log-likelihood [14].

The comparison between two models will be based on the Akaike information criterion (AIC), which is defined as $\text{AIC}=-2\ln\hat{L}+2k$, where $\ln\hat{L}$ is maximum log-likelihood for a given model, k is number of parameters in the model, and the additional factor of 2 is just a sop to historical precedents. This represents a rough way of compensating for the effect of adding parameters and is a useful heuristic measure of the relative effectiveness of different models. Thus, in comparing the stick-slip (or stress release) model with three parameters against the Poisson model with only one parameter $[\nu=\rho=0$ in Eq. (3a)], the former must demonstrate a significantly better fit to justify the additional parameters. Hence the relative effectiveness of two models in fitting the AE data can be assessed by the difference of their AIC values, $\Delta\text{AIC}=\text{AIC}_\text{P}-\text{AIC}_\text{s}$, where AIC_P and AIC_s represent the AIC values of the Poisson and stick-slip models, respectively [15,16]. As listed in Table I, if we take the Poisson model (random process) as a reference, it is obvious to see that the stick-slip model fits the AE data better than the Poisson model at 400 °C since the difference of the AIC values is substantial—that is, $\Delta\text{AIC}>2$. However, such a direct comparison might be misleading, as the coatings deposited at different temperatures yield very different numbers of AE events (see Table I). To allow for this effect, we use the indicator $\Delta\text{AIC}/N$ as a measure of the improvement in performance, which is approximately independent of sample

TABLE I. AIC values calculated by using the Poisson model (AIC_P) and statistical stick-slip model (AIC_s) to samples deposited at various temperatures, where $\Delta\text{AIC}=\text{AIC}_\text{P}-\text{AIC}_\text{s}$ and N is number of AE events with magnitude $m\geqslant 60$ dB covering the time period from 25 to 36 s.

Samples	N	AIC_P	AIC_s	ΔAIC	$\Delta\text{AIC}/N$
Without heating	156	−514.012	−512.309	−1.703	−0.0109
400 °C	81	−160.909	−163.210	2.301	0.0284
500 °C	130	−379.779	−379.814	0.035	0.0003
600 °C	161	−551.090	−551.503	0.413	0.0026

TABLE II. Fitted parameters by using the statistical stick-slip model, as formulated in Eq. (3), to samples deposited at various deposition temperatures.

		Equation (3a)			Equation (3b)		
Samples	N	α	ν	ρ	t_0	S_0	η
Without heating	156	2.50	0.45	1.02	0.63	0.58	0.19
400 °C	81	1.38	0.50	0.73	0.71	1.96	0.99
500 °C	130	2.25	0.25	1.67	0.60	1.00	0.27
600 °C	161	2.29	0.26	1.45	0.43	0.62	0.19

size [12]. The same trend of changes (400, 600, 500 °C and without heating) was obtained, and the best fit is still the case of 400 °C. Here it is worth noting that the relatively small increase of $\Delta\mathrm{AIC}/N$ values for 500 and 600° C might be caused by the instability of mechanical properties of the coatings at these high deposition temperatures [17]. Here the larger the ratio of $\Delta\mathrm{AIC}/N$, the better the AE data are fitted by the statistical stick-slip model relative to the Poisson model, and the more stable or optimal the coating. The fitted parameters in Eqs. (3a) and (3b) are set out in Table II, and the intensity function versus time for each deposition temperature is shown in Fig. 2. For a given stress release S_0, the larger the value η, the higher the sensitivity to risk ν ($\eta = \nu S_0$). The results also indicate that the coating deposited at 400 °C is more stable than those in the other three cases.

Nanoindentation experiments [18] showed that the coating (8.6 at. % Si) deposited at 400 °C has a hardness of 50.9 GPa, which was indeed larger than those with the same composition but deposited at different temperatures. Further, wear testing on these coatings was assessed. The drills coated with nc-TiN/a-Si_3N_4 deposited at 25 °C (without heating), 400 °C, 500 °C, and 600 °C drilled 78, 352, 120, and 225 holes, respectively. For comparison, the drill coated with TiN (hardness $H \approx 20$ GPa), a commonly used hard coating, drilled only 107 holes [19].

It is interesting to scrutinize the AE data at 400 °C, the optimal deposition temperature obtained from the statistical analysis and real-life testing. As shown in Fig. 3, the magnitude-frequency distribution of AE events follows, $\log_{10} N\,(>m) = -km + \mathrm{const}$, with $k = 0.026 \pm 0.001$, a relationship similar to the Gutenberg-Richter law, $\log_{10} N\,(>M) = -bM + \mathrm{const}$, in seismology, where M is the magnitude of an earthquake and the so-called seismic b value is approximately within the interval $0.5 \leqslant b \leqslant 1.2$. As is well known, the Gutenberg-Richter law can be represented as a power-law distribution $N\,(>E) \sim E^{-2b/3}$, where E is energy released in an earthquake [20]. Since the energy released in an AE event is approximately proportional to its power, in terms of the magnitude definition of AE [see Eq. (2)], a similar power-law distribution $N\,(>E) \sim E^{-10k}$ is obtained. Then we have $2b/3 = 10k$—i.e., $b = 15k \approx 0.4$—which is about the b value for deep earthquakes. However, as the deposition temperature decreases or increases, the energy frequency of AE events deviates rapidly from the power-law distribution [21].

This universal power-law distribution over many scales implies that the behavior of the superhard coatings is likely to be independent of microscopic and macroscopic details, and the understanding of their mechanical behavior may depend on only a few emergent material parameters as was done in the model. As crystalline gain sizes are reduced to the nanometer scale, the percentage of grain boundary atoms increases rapidly (about 10% of atoms are located at grain

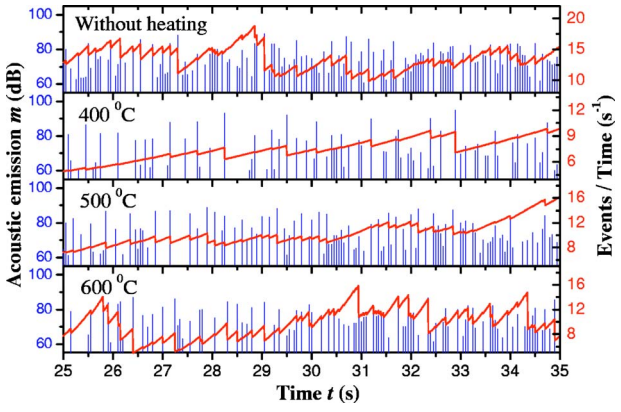

FIG. 2. (Color online) The risk level (the number of events per second) vs time calculated by the fitted parameters in Eq. (3a). For comparison, the AE events with magnitude $m \geqslant 60$ dB are also shown.

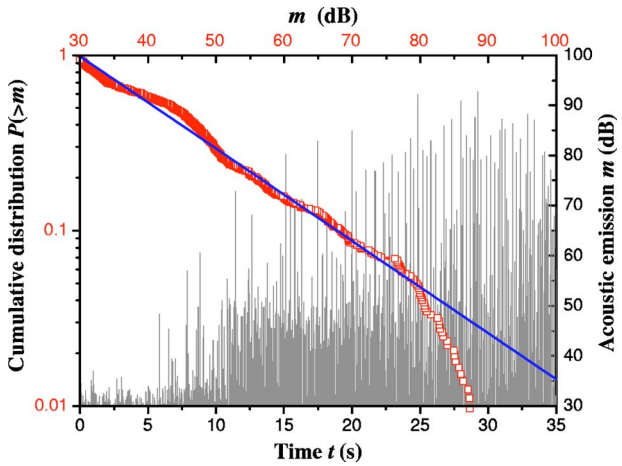

FIG. 3. (Color online) AE signals from scratching test of nc-TiN/a-Si_3N_4 coatings (8.6 at. % Si and 400 °C deposition temperature) vs time and cumulative frequency-magnitude distribution $P\,(>m)$ of AE events with magnitude greater than m, where the slope of solid line is −0.026. Here $P\,(>m) = N\,(>m)/N$, and N is total number of AE events.

boundaries for a sample with grain diameters of 20 nm) [22]. Compared with coarse-grained metals, there are different deformation mechanisms and most of which occur and compete in mechanically loaded nanocrystalline materials. Owing to the competition between different deformation forms such as dislocation pileups in nanocrystalline grains and grain sliding (and grain rotation) within the amorphous boundary, a steady self-organized nanostructure with peculiar properties (such as superhardness) can be formed. This may be a possible reason that the AE events due to scratching occur similarly on different sizes when the nanostructure of a coating lies in an optimal state [5]. Such a special kind of self-organized nanostructure is often necessary for a superhard material. For example, three correlative conditions for a superhard covalent crystal should be met: higher bond density or electronic density, shorter bond length, and greater degree of covalent bonding [23].

In summary, optimum information, such as Si content, deposition temperature, etc., in nc-TiN/a-Si_3N_4 coatings can be extracted from the crackling noise by using a simple stick-slip model. As the nanostructure of a coating approaches an optimal state, the frequency-magnitude distribution of AE energy follows the power-law statistics. The results provide us valuable clues to understand the superhardening mechanisms of nanocomposite coatings and, further, to tailor new nanostructural coatings with superhardness. Since earthquakes and even price fluctuations in stock markets can be viewed as a special kind of crackling noise, the present method may be easily extended to the prediction of these phenomena.

We are grateful to C. H. Zhang for providing the AE data and D. Vere-Jones for valuable discussions. This work was supported by the Australian Research Council (ARC) and the Research Grants Council of the Hong Kong SAR, China (Grant No. 1097/02E).

[1] For a recent review on crackling noise, see J. P. Sethna, K. A. Dahmen, and C. R. Myers, Nature (London) **410**, 242 (2001), and references therein.

[2] G. Galdarelli, F. D. di Tolla, and A. Petri, Phys. Rev. Lett. **77**, 2503 (1996); A. Garcimartin *et al.*, *ibid.* **79**, 3202 (1997); A. Guarino, A. Garcimartin, and S. Ciliberto, Eur. Phys. J. B **6**, 13 (1998).

[3] S. Zapperi, P. Ray, H. E. Stanley, and A. Vespignani, Phys. Rev. Lett. **78**, 1408 (1997); S. Zapperi, A. Vespignani, and H. E. Stanley, Nature (London) **388**, 658 (1997).

[4] L. I. Salminen, A. I. Tolvanen, and M. J. Alava, Phys. Rev. Lett. **89**, 185503 (2002); M. Koslowski, R. LeSar, and R. Thomson, *ibid.* **93**, 125502 (2004).

[5] P. Bak, C. Tang, and K. Wiesenfeld, Phys. Rev. Lett. **59**, 381 (1987); D. L. Turcotte, Rep. Prog. Phys. **62**, 1377 (1999).

[6] S. Vepřek, J. Vac. Sci. Technol. A **17**, 2401 (1999); S. Vepřek and A. S. Argon, J. Vac. Sci. Technol. B **20**, 650 (2002).

[7] B. Bhushan, J. N. Isrealachvili, and U. Landman, Nature (London) **374**, 607 (1995), and references therein.

[8] P. Hedenqvist and S. Hogmark, Tribol. Int. **30**, 507 (1997); J. von Stebut *et al.*, Surf. Coat. Technol. **116–119**, 160 (1999).

[9] M. Urabakh *et al.*, Nature (London) **430**, 525 (2004), and references therein.

[10] N. J. Persson, *Sliding Friction: Physical Principles and Applications*, 2nd ed. (Springer, Berlin, 2000).

[11] E. Bouchaud, J. Phys.: Condens. Matter **9**, 4319 (1997), and references therein; F. Célarié *et al.*, Phys. Rev. Lett. **90**, 075504 (2003).

[12] D. Vere-Jones, J. Phys. Earth **26**, 129 (1978); X. Zheng and D. Vere-Jones, Pure Appl. Geophys. **135**, 559 (1991); C. Lu, D. Vere-Jones, and H. Takayasu, Phys. Rev. Lett. **82**, 347 (1999); C. Lu and D. Vere-Jones, J. Geophys. Res. **106**, 11115 (2001).

[13] Provided that there was an ideal material, $\psi(\sigma)$ would be zero until σ reached the critical strength and infinite beyond it. By contrast, a finite constant value of $\psi(\sigma)$ corresponds to a pure random process where the occurrence of AE events is independent of stress level. Thus an exponential function is a convenient compromise between the two extreme cases.

[14] The log-likelihood of a risk function is defined as $\ln L = \sum_{i=1}^{N} \ln \lambda(t_i) - \int_{t_1}^{t_2} \lambda(t) dt$. The independence assumption allows the likelihood to be written as the product of two terms, the likelihood for times, taking the observed stress drops as given, and for stress drops, which reduces to the standard form for a set of independent, identically distributed values.

[15] H. Akaike, IEEE Trans. Autom. Control **19**, 716 (1974); Y. Sakamoto, M. Ishiguro, and G. Kitagawa, *Akaike Information Criterion Statistics* (Reidel, Dordrecht, 1983). In typical cases, the difference between two models which would be significant at around the 5% confidence level corresponds to the difference in AIC values of 1.5–2.

[16] C. Lu, R. Danzer, and F. D. Fischer, Phys. Rev. E **65**, 067102 (2002); J. Eur. Ceram. Soc. **24**, 3643 (2004).

[17] Experimental results showed that the mechanical properties like hardness of coatings become unstable at high deposition temperatures. Although we cannot absolutely judge what happens at temperatures larger than 600 °C according to the data on hand, it seems that the $\Delta \mathrm{AIC}/N$ values might decrease.

[18] W. C. Oliver and G. M. Pharr, J. Mater. Res. **7**, 1564 (1992); **19**, 3 (2004).

[19] Here the machining precision does not change; i.e., the tolerance and roundness of the holes drilled by coated drills were similar to those of holes drilled by uncoated drills.

[20] B. Gutenberg and C. F. Richter, *Seismicity of the Earth and Associated Phenomena* (Princeton University Press, Princeton, 1954); I. Main, Rev. Geophys. **34**, 433 (1996).

[21] Due to the lack of data on microstructural distributions, the scaling function could not be found by collapsing the data from different deposition temperatures onto one curve. Work on an underlying phase transition in this process is in progress.

[22] J. Schiotz, F. D. Di Tolla, and K. W. Jacobsen, Nature (London) **391**, 561 (1998); H. Van Swygenhoven, Science **296**, 66 (2002); J. Schiotz and K. W. Jacobsen, *ibid.* **301**, 1357 (2003).

[23] F. Gao *et al.*, Phys. Rev. Lett. **91**, 015502 (2003); Z.-J. Liu, P. W. Shum, and Y. G. Shen, Thin Solid Films **468**, 161 (2004).